The Structure of the Other Rotamer of Formic Acid, *cis*-HCOOH [1, 2]

E. Bjarnov and W. H. Hocking *
Physikalisch-Chemisches Institut, Justus-Liebig-Universität, Gießen
and
Max-Planck-Institut für Radioastronomie, Bonn, B.R.D.

Z. Naturforsch. **33a**, 610–618 (1978); received February 26, 1978

The very weak microwave spectra of six isotopically substituted species of formic acid in the *cis* rotamer form (i.e. with the two hydrogen atoms *cis* to each other) have been studied. From the data on $HC^{18}OOH$, $HCO^{18}OH$, $H^{13}COOH$, HCOOD, DCOOH and DCOOD, together with the previously published data for HCOOH, the complete substitution structure of the *cis* rotamer of formic acid has been derived. The structure is: $r_s(C-H) = 1.105(4)$ Å, $r_s(C{=}O) = 1.195(3)$ Å, $r_s(C-O) = 1.352(3)$ Å, $r_s(O-H) = 0.956(5)$ Å, $\sphericalangle_s(OCO) = 122.1(4)°$, $\sphericalangle_s(HC-O) = 114.6(6)°$ and $\sphericalangle_s(COH) = 109.7(4)°$.

I. Introduction

Formic acid is one of the simplest molecules that can exhibit rotational isomerism. Two planar rotameric forms are possible:

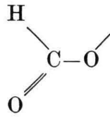

cis

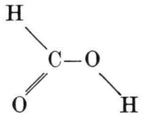

trans

Numerous experimental studies [1] have shown the *trans* rotamer to be the predominant naturally occuring form, but, from *ab initio* calculations [1, 2], a potential minimum is also expected at the *cis* configuration.

In a recent paper Hocking [3] reported the unequivocal identification of the *cis* rotamer of formic acid through assignment of its microwave spectrum. Although there had been several tentative assignments of a few infrared absorption bands to the *cis* rotamer [4, 5], prior to Ref. [3] *cis*-HCOOH had not been positively identified.

In Ref. [3] the energy difference between the ground vibrational states of the two rotamers of formic acid was determined from measurements of the relative intensities of the microwave transitions. The *cis* rotamer was found to lie at higher energy than the *trans* rotamer by 1365 ± 30 cm^{-1}. Furthermore the electric dipole moment of *cis*-HCOOH in its vibrational ground state was determined to be 3.79 D, whereas for the *trans* rotamer 1.42 D had been found [6].

In view of the importance of formic acid, both as the parent member of the carboxylic acid homologous series and as a test of theoretical models of intramolecular forces, it seemed to us worthwhile to determine accurately the structure of the *cis* rotamer. Furthermore, since formic acid is known to be present in interstellar clouds [7], we felt it valuable to provide data that could be used for the identification of the *cis* rotamer of isotopically substituted formic acid in space. Accordingly we have measured and analysed the very weak microwave spectra of six isotopically substituted species of the *cis* rotamer of formic acid: $HC^{18}OOH$, $HCO^{18}OH$, $H^{13}COOH$, HCOOD, DCOOH, and DCOOD. These data have allowed the determination of a complete substitution structure for *cis*-HCOOH. The differences between the structures of the two rotamers of formic acid are discussed in terms of non-bonded forces.

II. Experimental Procedures

Isotopically enriched samples of formic acid were obtained from commercial sources as follows: $H^{13}COOH$ (90 atom% ^{13}C) and DCOOH (98 atom% D) from Merck, Sharp and Dohme Canada Limited and ^{18}O-HCOOH (ca. 40 atom% ^{18}O) from Stohler Isotope Chemicals, Mass. USA. The commercial

---

[1] This work was supported in part by funds from the Deutsche Forschungsgemeinschaft.

[2] Presented in part at the "Fifth Colloquium on High Resolution Molecular Spectroscopy", Tours, France, September 19–23 (1977) as paper 013.

* Present address: Department of Chemistry, The University of British Columbia, Vancouver, B.C., Canada.

Reprint requests to Dr. E. Bjarnov, Physikalisch-Chemisches Institut, Justus-Liebig-Universität, Heinrich-Buff-Ring 58, D-6300 Lahn-Gießen.

products were used without further purification. HCOOD and DCOOD were prepared by adding deuterated orthophosphoric acid (99 atom% D from Merck, Sharp and Dohme Canada Ltd.) to the appropriate sodium salt and distilling off the labelled formic acid *in vacuo*.

All measurements were made at room temperature with ~ 15 mTorr pressure of formic acid in the microwave cell. The spectra in the 12.4—50 GHz region were recorded with a Hewlett-Packard 846OAMRR spectrometer as described in Ref. [3]. The uncertainty in the measured transition frequencies is estimated to be less than ± 50 kHz. A few lines were either too weak or over-lapped with other lines so that this accuracy in the measurement could not be achieved. These transitions were not used for the determination of the spectroscopic constants.

III. Rotational Spectra, Assignment and Analysis

The rotational spectra of the six isotopically labelled species of the *cis* rotamer of formic acid were assigned in the following way. Using the preliminary structure given in Ref. [3] the rotational constants of each isotopic species were calculated and the $1_{01}-0_{00}$ transition was predicted ($\nu = B + C$). A search of the spectrum of the appropriate sample then yielded this transition. Figure 1 shows the $1_{01}-0_{00}$ line for the six species. Next, the $J = 2 \leftarrow 1$ ***a***-type R branch transitions were searched for. In each case the $K_a = 0$ and both of the asymmetry-split $K_a = 1$ components were found. The above assignments were in most cases confirmed by the Stark effect of the microwave transitions. The third and most difficult step was to assign low J ***b***-type transitions. This required considerable searching and in some cases several alternative assignments were initially possible. The measured transition frequencies were used to calculate the rigid rotor rotational constants for each species. From the A, B and C constants based on the correct assignments and the quartic centrifugal distortion constants determined in Ref. [3] for the unsubstituted species the spectra could be predicted reasonably well up to $J \sim 25$. Additional ***a***-type Q-branchand ***b***-type P-branch transitions were then assigned in a systematic fashion following the bootstrap procedure [8]. The fact that lines due to the *cis* rotamer are approximately twice as broad as those of the *trans* rotamer was of considerable help in the assignment process. Eventually, between 20 and 26 transitions belonging to the ${}^qR_0$, ${}^qR_1$, ${}^qQ_1$, ${}^qQ_2$, ${}^qQ_3$, ${}^rP_0$, ${}^rP_1$, ${}^rP_2$, and ${}^rP_3$ branches were assigned for each isotopic species. The observed transition frequencies are collected in Tables 1 to 6.

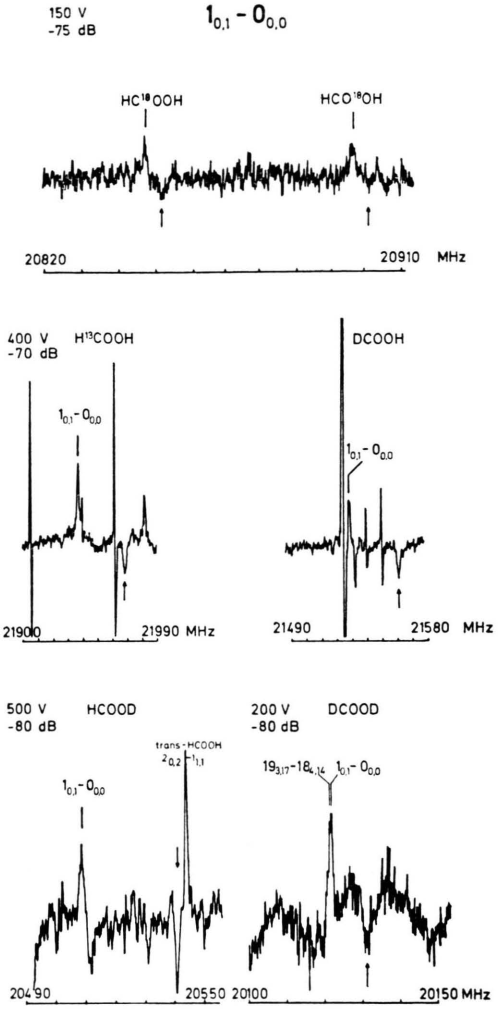

Fig. 1. Recorder tracings of the $1_{01}-0_{00}$ transitions of six isotopic species of the *cis* rotamer of formic acid. The arrows point at the Stark components.

The spectra were analysed using Watson's reduced Hamiltonian given in Ref. [3] Eq. (1) which includes centrifugal distortion terms up to fourth power in the angular momenta. An iterative least squares procedure was used to fit the observed spectra to this Hamiltonian. A few transitions involving high values of J and K_a were omitted in

Table 1. Observed and calculated frequencies of *cis*-HC(:^{18}O)OH in MHz.

Transition	Observed frequency	Calculated frequency
a-type R-branch		
$1_{0,1} - 0_{0,0}$	20837.130	20837.184 (08)[a]
$2_{0,2} - 1_{0,1}$	41657.810	41657.807 (15)
$2_{1,2} - 1_{1,1}$	40394.710	40394.703 (17)
$2_{1,1} - 1_{1,0}$	42954.285	42954.257 (16)
a-type Q-branch		
$15_{2,13} - 15_{2,14}$	35216.580	35216.601 (27)
b-type P-branch		
$1_{1,1} - 2_{0,2}$	32669.840	32669.871 (23)
$5_{0,5} - 4_{1,4}$	35082.305	35082.304 (25)
$7_{2,6} - 8_{1,7}$	35740.84[b]	35740.754 (48)
$11_{1,10} - 10_{2,9}$	44651.20[b]	44651.184 (49)
$11_{2,9} - 12_{1,12}$	38010.230	38010.210 (21)
$12_{2,10} - 13_{1,13}$	30370.020	30369.988 (18)
$13_{2,11} - 14_{1,14}$	24486.570	24486.608 (26)
$14_{3,12} - 15_{2,13}$	36369.870	36369.862 (28)
$17_{2,15} - 16_{3,14}$	18881.330	18881.316 (30)
$16_{3,13} - 17_{2,16}$	39071.460	39071.456 (21)
$17_{3,14} - 18_{2,17}$	23272.990	23272.995 (23)
$22_{2,21} - 21_{3,18}$	28614.140	28614.130 (20)
$23_{2,22} - 22_{3,19}$	38079.230	38079.256 (18)
$24_{2,23} - 23_{3,20}$	45870.100	45870.089 (27)
$21_{4,18} - 22_{3,19}$	43024.810[c]	43025.14 (18)
$23_{4,19} - 24_{3,22}$	25262.670[c]	25263.14 (13)

[a] One standard error in units of the last digit.

[b] Not included in the fit due to limited measuring accuracy.

[c] Not included in the fit in order to avoid higher order effects.

Table 2. Observed and calculated frequencies of *cis*-H(:O)^{18}OH in MHz.

Transition	Observed frequency	Calculated frequency
a-type R-branch		
$1_{0,1} - 0_{0,0}$	20897.000	20897.019 (06)[a]
$2_{0,2} - 1_{0,1}$	41777.120	41777.148 (13)
$2_{1,2} - 1_{1,1}$	40503.960	40503.903 (14)
$2_{1,1} - 1_{1,0}$	43084.320	43084.352 (14)
a-type Q-branch		
$7_{1,6} - 7_{1,7}$	36091.160	36091.155 (17)
$15_{2,13} - 15_{2,14}$	35838.300	35838.312 (16)
b-type P-branch		
$1_{1,1} - 2_{0,2}$	32302.32[b]	32302.382 (13)
$5_{0,5} - 4_{1,4}$	35666.185	35666.165 (12)
$7_{2,6} - 8_{1,7}$	34357.690	34357.702 (21)
$11_{1,10} - 10_{2,9}$	46342.945	46342.955 (19)
$10_{2,8} - 11_{1,11}$	46432.86[b]	46432.939 (17)
$11_{2,9} - 12_{1,12}$	37219.680	37219.651 (18)
$12_{2,10} - 13_{1,13}$	29674.050	29674.063 (19)
$19_{2,17} - 20_{1,20}$	30425.290	30425.308 (18)
$20_{2,18} - 21_{1,21}$	38534.220	38534.207 (23)
$14_{3,12} - 15_{2,13}$	33813.430	33813.421 (24)
$17_{2,15} - 16_{3,14}$	21751.390	21751.397 (24)
$16_{3,13} - 17_{2,16}$	37223.880	37223.882 (24)
$22_{2,21} - 21_{3,18}$	29996.550	29996.550 (19)
$23_{2,22} - 22_{3,19}$	39287.050	39287.053 (24)
$21_{4,18} - 22_{3,19}$	39452.860[c]	39453.204 (94)
$22_{4,18} - 23_{3,21}$	41904.960[c]	41905.311 (80)
$23_{4,19} - 24_{3,22}$	22315.530[c]	22315.908 (78)

[a–c] See Table 1 for footnotes.

Table 3. Observed and calculated frequencies of *cis*-H^{13}COOH in MHz.

Transition	Observed frequency	Calculated frequency
a-type R-branch		
$1_{0,1} - 0_{0,0}$	21937.140	21937.153 (05)[a]
$2_{0,2} - 1_{0,1}$	43852.980	43852.944 (11)
$2_{1,2} - 1_{1,1}$	42436.780	42436.735 (12)
$2_{1,1} - 1_{1,0}$	45312.010	45312.043 (12)
a-type Q-branch		
$5_{1,4} - 5_{1,5}$	21557.440	21557.452 (08)
$6_{1,5} - 6_{1,6}$	30170.280	30170.269 (11)
$11_{2,9} - 11_{2,10}$	14471.810	14471.823 (06)
$12_{2,10} - 12_{2,11}$	19938.34[b]	19938.362 (08)
$13_{2,11} - 13_{2,12}$	26668.170	26668.160 (09)
$15_{2,13} - 15_{2,14}$	44285.760	44285.779 (14)
$21_{3,18} - 21_{3,19}$	23341.010[c]	23340.854 (28)
b-type P-branch		
$1_{1,1} - 2_{0,2}$	28659.250	28659.263 (08)
$6_{2,5} - 7_{1,6}$	46457.460	46457.468 (15)
$7_{2,6} - 8_{1,7}$	19064.160	19064.185 (13)
$10_{1,9} - 9_{2,8}$	37493.630	37493.664 (15)
$10_{2,8} - 11_{1,11}$	37819.860	37819.866 (10)
$11_{2,9} - 12_{1,12}$	29412.510	29412.513 (11)
$12_{2,10} - 13_{1,13}$	22962.070	22962.053 (12)
$13_{2,11} - 14_{1,14}$	18585.000	18585.001 (13)
$18_{2,16} - 19_{1,19}$	29994.31[b]	29994.291 (19)
$19_{2,17} - 20_{1,20}$	38986.280	38986.282 (23)
$13_{3,11} - 14_{2,12}$	33379.100	33379.086 (19)
$16_{2,14} - 15_{3,13}$	24954.970	24954.946 (18)
$15_{3,12} - 16_{2,15}$	33845.745	33845.734 (15)
$16_{3,13} - 17_{2,16}$	17367.970	17367.969 (16)
$20_{2,19} - 19_{3,16}$	24508.765	24508.756 (14)
$21_{2,20} - 20_{3,17}$	35401.990	35401.996 (20)
$20_{4,17} - 21_{3,18}$	26211.235[c]	26211.552 (69)

[a–c] See Table 1 for footnotes.

Table 4. Observed and calculated frequencies of *cis*-HCOOD in MHz.

Transition	Observed frequency	Calculated frequency
a-type R-branch		
$1_{0,1} - 0_{0,0}$	20508.79[b]	20508.856 (06)[a]
$2_{0,2} - 1_{0,1}$	41001.435	41001.430 (11)
$2_{1,2} - 1_{1,1}$	39758.890	39758.914 (12)
$2_{1,1} - 1_{1,0}$	42276.615	42276.573 (12)
a-type Q-branch		
$6_{1,5} - 6_{1,6}$	26421.53[b]	26421.556 (15)
$7_{1,6} - 7_{1,7}$	35214.450	35214.457 (15)
$14_{2,12} - 14_{2,13}$	27073.195	27073.200 (13)
$15_{2,13} - 15_{2,14}$	34662.850	34662.845 (14)
b-type P-branch		
$1_{1,1} - 2_{0,2}$	32075.570	32075.598 (11)
$5_{0,5} - 4_{1,4}$	34606.280	34606.284 (11)
$7_{2,6} - 8_{1,7}$	34950.630	34950.642 (17)
$11_{1,10} - 10_{2,9}$	44169.980	44169.991 (19)
$10_{2,8} - 11_{1,11}$	46281.920	46281.880 (12)
$11_{2,9} - 12_{1,12}$	37135.590	37135.579 (12)
$12_{2,10} - 13_{1,13}$	29609.350	29609.372 (13)
$13_{2,11} - 14_{1,14}$	23812.060	23812.078 (14)
$19_{2,17} - 20_{1,20}$	29086.980	29086.982 (17)
$20_{2,18} - 21_{1,21}$	36825.570	36825.566 (21)
$14_{3,12} - 15_{2,13}$	35387.320	35387.329 (22)
$17_{2,15} - 16_{3,14}$	19004.295	19004.282 (15)
$16_{3,13} - 17_{2,16}$	38041.295	38041.262 (16)
$18_{2,16} - 17_{3,15}$	47436.010	47436.024 (22)
$17_{3,14} - 18_{2,17}$	22488.360	22488.386 (19)
$29_{5,24} - 30_{4,27}$	37050.230[c]	37051.51 (16)

[a–c] See Table 1 for footnotes.

Table 5. Observed and calculated frequencies of *cis*-DCOOH in MHz.

Transition	Observed frequency	Calculated frequency
a-type R-branch		
$1_{0,1} - 0_{0,0}$	21528.060	21528.052 (04)[a]
$2_{0,2} - 1_{0,1}$	43006.42[b]	43006.352 (07)
$2_{1,2} - 1_{1,1}$	41203.970	41203.955 (08)
$2_{1,1} - 1_{1,0}$	44908.050	44908.058 (07)
a-type Q-branch		
$4_{1,3} - 4_{1,4}$	18513.920	18513.914 (05)
$6_{1,5} - 6_{1,6}$	38818.900	38818.877 (06)
$10_{2,8} - 10_{2,9}$	22347.870	22347.873 (06)
$11_{2,9} - 11_{2,10}$	31194.300	31194.302 (06)
$16_{3,13} - 16_{3,14}$	19766.3[b]	19766.207 (09)
$18_{3,15} - 18_{3,16}$	36572.920	36572.913 (13)
b-type P-branch		
$4_{0,4} - 3_{1,3}$	39067.240	39067.238 (07)
$4_{2,3} - 5_{1,4}$	34449.280	34449.295 (08)
$7_{1,6} - 6_{2.5}$	19843.210	19843.229 (07)
$6_{2,4} - 7_{1,7}$	35249.030	35249.049 (07)
$7_{2,5} - 8_{1,8}$	24301.160	24301.148 (09)
$8_{2,6} - 9_{1,9}$	15643.81[b]	15643.809 (12)
$9_{3,7} - 10_{2,8}$	27324.300	27324.310 (08)
$10_{3,7} - 11_{2,10}$	32035.950	32035.942 (06)
$12_{2,10} - 11_{3,9}$	29658.030	29658.046 (08)
$14_{2,13} - 13_{3,10}$	15712.410	15712.387 (07)
$15_{2,14} - 14_{3,11}$	28273.590	28273.604 (07)
$16_{2,15} - 15_{3,12}$	38677.735	38677.731 (13)
$14_{4,10} - 15_{3,13}$	38254.820	38254.817 (10)
$14_{4,11} - 15_{3,12}$	23833.510	23833.512 (11)
$15_{4,11} - 16_{3,14}$	17423.430	17423.433 (07)
$17_{3,14} - 16_{4,13}$	31486.630	31486.632 (11)
$18_{3,16} - 17_{4,13}$	22396.310	22396.310 (12)
$22_{4,18} - 21_{5,17}$	32786.960[c]	32786.709 (31)
$22_{4,19} - 21_{5,16}$	16720.360[c]	16720.174 (23)
$23_{4,20} - 22_{5,17}$	38518.880[c]	38518.664 (32)
$23_{6,18} - 24_{5,19}$	38965.530[c]	38965.920 (61)

[a–c] See Table 1 for footnotes.

Table 6. Observed and calculated frequencies of *cis*-DCOOD in MHz.

Transition	Observed frequency	Calculated frequency
a-type R-branch		
$1_{0,1} - 0_{0.0}$	20121.75[b]	20121.519 (04)[a]
$2_{0,2} - 1_{0,1}$	40203.360	40203.335 (08)
$2_{1,2} - 1_{1,1}$	38595.615	38595.586 (08)
$2_{1,1} - 1_{1,0}$	41890.305	41890.310 (08)
a-type Q-branch		
$5_{1,4} - 5_{1,5}$	24692.23[b]	24692.193 (08)
$6_{1,5} - 6_{1,6}$	34541.300	34541.312 (10)
$11_{2,9} - 11_{2,10}$	25433.98[b]	25433.973 (07)
$12_{2,10} - 12_{2,11}$	34400.940	34400.935 (08)
$13_{2,11} - 13_{2,12}$	45090.050	45090.029 (12)
$19_{3,16} - 19_{3,17}$	36054.83[b]	36054.773 (27)
b-type P-branch		
$4_{0,4} - 3_{1,3}$	33413.330	33413.344 (07)
$4_{2,3} - 5_{1,4}$	41623.370	41623.382 (12)
$6_{2,4} - 7_{1,7}$	40035.805	40035.816 (09)
$8_{1,7} - 7_{2,6}$	34838.505	34838.494 (10)
$7_{2,5} - 8_{1,8}$	29059.430	29059.447 (09)
$8_{2,6} - 9_{1,9}$	20024.460	20024.445 (11)
$15_{2,13} - 16_{1,16}$	24303.26[b]	24303.146 (17)
$16_{2,14} - 17_{1,17}$	35045.700	35045.703 (19)
$11_{3,8} - 12_{2,11}$	26536.645	26536.657 (10)
$13_{2,11} - 12_{3,10}$	37195.065	37195.092 (11)
$16_{2,15} - 15_{3,12}$	28139.685	28139.689 (09)
$17_{2,16} - 16_{3,13}$	37512.685	37512.701 (16)
$15_{4,11} - 16_{3,14}$	36370.430	36370.428 (15)
$15_{4,12} - 16_{3,13}$	21300.100	21300.096 (14)
$18_{3,15} - 17_{4,14}$	30628.340	30628.342 (17)
$19_{3,17} - 18_{4,14}$	20121.75[b]	20121.784 (17)
$20_{3,18} - 19_{4,15}$	37508.840	37508.821 (16)

[a–c] See Table 1 for footnotes.

the fitting procedures in order to avoid higher order effects. The spectroscopic constants thus obtained are given in Table 7.

The constants reported in Tables 8 and 9 were derived from the spectroscopic constants (Table 7). Table 8 gives Watson's determinable constants [9, 10] and Table 9 the constants obtained by applying the planarity constraints [10].

IV. Molecular Structure

The Kivelson and Wilson [11] rotational constants in Table 9 were used for the determination of the molecular structure since they contain no centrifugal distortion contributions. The moments of inertia given in Table 10 were calculated from these constants using the conversion factor $B \cdot I_b = 505379.0\ (38)\ \text{MHz} \cdot \text{u} \cdot \text{Å}^2$. The small positive values of the inertial defect confirm that the *cis* rotamer of formic acid is planar.

The substitution structure of the planar *cis* formic acid can be obtained from three sets of moments of intertia, (I_b, I_c), (I_a, I_b) and (I_a, I_c),

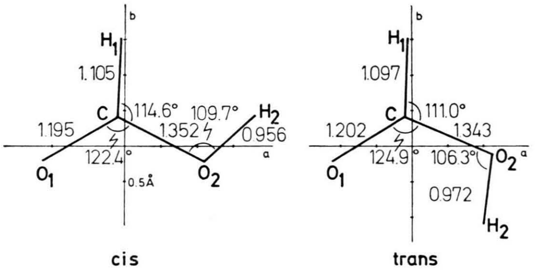

Fig. 2. Molecular structures of *cis*- and *trans*-HCOOH. The *trans* structure is that given by Kwei and Curl [12]. The numbering of the atoms is given by indices.

Table 7. Spectroscopic constants of seven isotopic species of *cis* formic acid[a].

	HCOOH[b]	HC(:^{18}O)OH	HC(:O)^{18}OH	H^{13}COOH	HCOOD	DCOOH	DCOOD	
$\tilde{A}$	86461.565 (22)	85388.388 (35)	85175.320 (26)	84201.819 (19)	83962.785 (22)	62653.4395 (87)	61507.409 (11)	MHz
$\tilde{B}$	11689.1767 (30)	11058.5903 (40)	11093.7328 (33)	11687.5239 (28)	10883.9413 (29)	11690.1692 (18)	10884.5356 (22)	MHz
$\tilde{C}$	10283.9868 (30)	9778.6232 (40)	9803.3164 (33)	10249.6623 (28)	9624.9421 (29)	9837.9145 (18)	9237.0082 (22)	MHz
Δ_J	8.353 (35)	7.428 (52)	7.682 (28)	8.268 (23)	6.733 (36)	7.899 (29)	6.267 (29)	kHz
Δ_{JK}	−71.07 (77)	−72.7 (12)	−68.72 (67)	−70.26 (52)	−48.11 (81)	−22.94 (48)	−15.25 (48)	kHz
Δ_K	2357.2 (45)	2345.2 (70)	2276.6 (47)	2315.0 (32)	1984.4 (48)	954.4 (11)	848.5 (14)	kHz
δ_J	1.4185 (22)	1.2334 (47)	1.2626 (17)	1.4433 (15)	1.0628 (21)	1.6633 (34)	1.2429 (23)	kHz
δ_K	41.102 (82)	37.55 (20)	37.936 (91)	40.431 (69)	33.911 (68)	37.541 (94)	31.315 (78)	kHz
σ[c]	25.5	31.9	28.0	23.4	25.1	14.3	19.1	kHz
N[d]	22	17	18	24	21	24	21	

[a] Numbers in parentheses are standard errors in units of the last digit.

[b] From Hocking [3].

[c] Standard deviation of the fit.

[d] Number of equally weighted transitions included in the fit.

Table 8. Watson's determinable rotational constants and quartic distortion constants for seven isotopic species of *cis* formic acid[a, b].

	HCOOH	HC(:^{18}O)OH	HC(:O)^{18}OH	H^{13}COOH	HCOOD	DCOOH	DCOOD	
$\mathfrak{A}$	86461.582 (22)	85388.403 (35)	85175.335 (26)	84201.836 (19)	83962.798 (22)	62653.4553 (87)	61507.422 (11)	MHz
$\mathfrak{B}$	11689.0373 (31)	11058.4549 (42)	11093.6011 (34)	11687.3864 (29)	10883.8367 (30)	11690.0837 (19)	10884.4678 (23)	MHz
$\mathfrak{C}$	10284.0175 (31)	9778.6429 (42)	9803.3414 (34)	10249.6923 (29)	9624.9774 (30)	9837.9858 (19)	9237.0706 (23)	MHz
τ'_{aaaa}	−9178 (18)	−9120 (28)	−8862 (19)	−9012 (13)	−7772 (19)	−3757.4 (48)	−3358.1 (59)	kHz
τ'_{bbbb}	−44.76 (14)	−39.58 (21)	−40.83 (11)	−44.618 (93)	−35.43 (14)	−44.90 (12)	−35.01 (12)	kHz
τ'_{cccc}	−22.06 (14)	−19.84 (21)	−20.63 (11)	−21.526 (93)	−18.43 (14)	−18.29 (12)	−15.12 (12)	kHz
τ_1	184.0 (31)	201.7 (48)	182.7 (27)	181.8 (21)	111.6 (33)	− 3.0 (20)	−14.2 (20)	kHz
τ_2'	−2.41 (34)	−0.69 (51)	−1.74 (29)	−1.76 (23)	−6.36 (35)	−16.41 (27)	−14.92 (26)	kHz
$\Delta\tau'_{cccc}$	−0.123 (41)	−0.146 (66)	−0.101 (32)	−0.142 (28)	−0.098 (40)	− 0.106 (48)	− 0.112 (42)	kHz

[a] The numbers in parentheses are standard errors in units of the last digit.

[b] $\tau_2' = \tau_2/(\alpha + \beta + \gamma)$; where α, β and γ are the rotational constants defined by Kivelson and Wilson [11]. See also Refs. [9] and [10].

Table 9. Rotational constants and quartic centrifugal distortion constants[a] derived from the planarity relations for seven isotopic species of *cis* formic acid.

	HCOOH	HC(:^{18}O)OH	HC(:O)^{18}OH	H^{13}COOH	HCOOD	DCOOH	DCOOD	
α'	86461.52	85388.35	85175.28	84201.77	83962.75	62653.39	61507.37	MHz
β'	11689.041	11058.466	11093.609	11687.389	10883.833	11690.053	10884.441	MHz
γ'	10284.144	9778.767	9803.461	10249.819	9625.069	9838.054	9237.123	MHz
$\hbar^4 \tau_{aabb}$	301.0	288.8	281.7	300.4	223.1	186.6	146.0	kHz
$\hbar^4 \tau_{bbcc}$	−30.39	−27.16	−28.15	−29.87	−24.78	−27.20	−21.92	kHz
$\hbar^4 \tau_{ccaa}$	103.13	106.25	102.55	97.51	72.33	39.54	29.43	kHz
$\hbar^4 \tau_{abab}$	−94.8	−83.1	−86.7	−93.1	−79.5	−101.0	−83.9	kHz

[a] Calculated using the planarity relations as described in Ref. [10], case 1.

Table 10. Moments of inertia and inertial defect of seven isotopic species of *cis* formic acid[a], [b].

	I_a	I_b	I_c	Δ
HCOOH	5.845132	43.23528	49.14157	0.06116
HC(:^{18}O)OH	5.918594	45.70064	51.68126	0.06203
HC(:O)^{18}OH	5.933400	45.55587	51.55108	0.06181
H^{13}COOH	6.001999	43.24140	49.30614	0.06274
HCOOD	6.019086	46.43392	52.50653	0.05352
DCOOH	8.066267	43.23154	51.36981	0.07200
DCOOD	8.216560	46.43133	54.71173	0.06384

[a] All constants are for the ground vibrational state in units of u · Å^2.

[b] $\Delta = I_c - I_a - I_b$.

using the planarity condition $I_c = I_a + I_b$ and Kraitchman's equations [14] for a planar molecule. The structure of *trans*-HCOOH has been determined from the *b*- and *c*-moments of inertia [12, 13]. To facilitate comparison between the two rotamers, the derivation of the structure of *cis*-HCOOH based on the (I_b, I_c) set will be given here. From Kraitchman's equations the *a*-coordinate of H_1, $a_{\mathrm{H}1}$ (see Fig. 2 for numbering of the atoms), was found to be imaginary, and the *a*-coordinate of C, a_{C}, was found to be 0.0788 Å, which is less than the minimum value (0.15 Å) that Costain [15] has suggested can be reliably determined from Kraitchman's equations. Accordingly these two coordinates were determined as follows: $a_{\mathrm{H}1}$ was fixed using the double substitution method of Krisher and Pierce [16] on the isotope pairs (DCOOH, HCOOH) and (DCOOD, HCOOD). The relations between the principal axis systems of HCOOD and HCOOH were calculated using the coordinates found from Kraitchman's equations with $a_{\mathrm{H}1}$ set equal to zero. The coordinate a_{C} was then determined using the center of mass condition $(\sum_i m_i a_i = 0)$. The final set of coordinates are given in Table 11 together with the coordinates determined in a similar way from (I_a, I_b) and (I_a, I_c).

The errors quoted were mostly determined using the ,,Constain rule'' [17]: $\delta r_{\mathrm{s}} = 0.0015/(r_{\mathrm{s}} \cdot \mu)$, with r_{s} being the substitution coordinate and μ the change in mass on substitution. The values obtained from Kraitchman's equations for the coordinates of the hydrogen atoms, using the different sets of moment of intertia data, differ in some cases by more than twice the error limits given by this rule. Similar changes have been found in the case of glyoxylic acid [18]. Consequently the errors quoted for these coordinates, $b_{\mathrm{H}1}$, $a_{\mathrm{H}2}$, and $b_{\mathrm{H}2}$, represent twice the error as calculated by the Costain rule. The error in $a_{\mathrm{H}1}$ was estimated from the variation of the value of this coordinate as calculated from the three different sets of moments of inertia. Finally the error in a_{C} was obtained by propagating the errors in the center of mass equation.

The structures calculated from the three sets of coordinates are also given in Table 11. The (I_b, I_c) structure of *cis*-HCOOH is compared with the structure of *trans*-HCOOH [12] in Fig. 2 and Table 12. There is at present less extensive data available for the ^{18}O species of the *trans* rotamer than for the *cis* rotamer, which limits the accuracy of the structure quoted for the former. The most recent structure reported for *trans*-HCOOH [19] was obtained by fitting the structural parameters to the moments of inertia of all isotopic species and, therefore, cannot be strictly compared with the *cis* structure presented here. In any case, it is nearly identical to the structure given by Kwei and Curl [12]. A somewhat different substitution structure has been reported for *trans*-HCOOH [13] which appears to involve the use of questionable values, obtained from Kraitchman's equations, for several small coordinates [19].

Table 11. Substitution coordinates and structures of *cis*-HCOOH as determined from three sets of moments of inertia[a, b].

	I_b, I_c	I_a, I_b	I_a, I_c	
a_{H_1}	−0.0475 (100)[c, d]	−0.0533[c]	−0.0296[c]	
a_C	−0.1018 (16)[d, e]	−0.1013[e]	−0.1030[e]	
a_{O_1}	−1.1319 (07)	−1.1319	−1.1321	
a_{O_2}	1.0979 (07)	1.0979	1.0981	
a_{H_2}	1.7983 (16)[f]	1.7981	1.7959	
b_{H_1}	1.5054 (20)[f]	1.5018	1.5020	
b_C	0.4017 (38)	0.3997	0.3997	
b_{O_1}	−0.2031 (37)	−0.2019	−0.2019	
b_{O_2}	−0.2218 (34)	−0.2209	−0.2209	
b_{H_2}	0.4282 (68)[f]	0.4379	0.4378	
$\sum_i m_i a_i$	0	0	0	u · Å
$\sum_i m_i b_i$	−0.0263	−0.0120	−0.0115	u · Å
$\sum_i m_i a_i b_i$	−0.0036	0.0029	0.0294	u · Å^2
$I_a^o - I_a^s$	−0.0069	0.0286	0.0281	u · Å^2
$I_b^o - I_b^s$	0.0781	0.0785	0.0712	u · Å^2
$I_c^o - I_c^s$	0.1320	0.1683	0.1604	u · Å^2
r_s (C—H$_1$)	1.1050 (43)	1.1031	1.1047	
r_s (C=O$_1$)	1.1945 (31)	1.1933	1.1920	
r_s (C—O$_2$)	1.3520 (28)	1.3503	1.3520	
r_s (O$_2$—H$_2$)	0.9555 (53)	0.9614	0.9597	
$\sphericalangle_s$ (O$_1$CO$_2$)	122.12 (37)	122.36	122.36	
$\sphericalangle_s$ (H$_1$CO$_2$)	114.64 (56)	114.87	113.52	
$\sphericalangle_s$ (CO$_2$H$_2$)	109.68 (44)	109.38	109.32	

[a] All coordinates are measured in Å units relative to the principal axis system of *cis*-HCOOH. Internuclear distances are given in Å units, angles in degrees.

[b] Errors are given in parentheses in units of the last digit. The error limits for the coordinates were estimated using the "Costain rule"[17], except where otherwise indicated. The errors in the structural parameters were obtained by propagating the errors quoted for the coordinates.

[c] This coordinate was determined by the double substitution method of Krisher and Pierce[16] using the planarity condition $I_c = I_a + I_b$. The error limit was estimated from the variation in the value found from the different sets of moments of inertia. Kraitchman's equations give an imaginary value for this coordinate using (I_b, I_c) or (I_a, I_b), but $a_{H_1} = -0.0824$ Å is obtained from (I_a, I_c).

[d] Simultaneous use of center of mass and product of inertia relations gives $a_{H_1} = -0.0436$ Å and $a_C = -0.1020$ Å.

[e] This coordinate was fixed using the center of mass relation. The error estimated was derived from the quoted uncertainties in the other a-coordinates. Kraitchman's equations give $a_C = -0.078$ (19) Å (I_b, I_c), $a_C = -0.079$ Å (I_a, I_b) and $a_C = -0.0884$ Å (I_a, I_c).

[f] These errors represent twice the "Costain rule"[17] estimate.

Table 12. Substitution structures of *cis*- and *trans*-HCOOH and differences between the structural parameters[a]. Differences between the two nonequivalent HCOO groups of formic anhydride[e] are presented for comparison.

	cis-HCOOH[b]	*trans*-HCOOH[c]	$r_{cis} - r_{trans}$	*trans*-HCOOH[d]	$r_{cis} - r_{trans}$	(CHO)$_2$O[e] $r_{\text{"}cis\text{"}} - r_{\text{"}trans\text{"}}$
r_s (C—H$_1$)	1.1050 (43)	1.097 (05)	0.0080 (66)	—[g]	—	0.003 (5)
r_s (C=O$_1$)	1.1945 (31)	1.202 (10)	−0.0075 (104)	1.201 (2)	−0.0065 (31)	−0.013 (4)
r_s (C—O$_2$)	1.3520 (28)	1.343 (10)	0.0090 (103)	1.343 (2)	0.0090 (34)	0.028 (9)
r_s (O$_2$ — H$_2$)	0.9555 (53)	0.972 (05)	−0.0165 (73)	0.971 (1)	−0.0155 (54)	—
$\sphericalangle_s$ (O$_1$CO$_2$)	122.12 (37)	124.9 (10)	−2.8 (11)	125.1 (2)[f]	−3.0 (4)	−5.3 (4)
$\sphericalangle_s$ (H$_1$C—O$_2$)	114.64 (56)	111.0 (20)[f]	3.6 (21)	110.8 (1)	3.8 (6)	3.7 (7)[f]
$\sphericalangle_s$ (CO$_2$H$_2$)	109.68 (44)	106.3 (10)	3.4 (11)	106.2 (1)	3.5 (5)	
$\sphericalangle_s$ (H$_1$C=O$_1$)	123.23 (58)	124.1 (20)	0.9 (21)	124.1 (2)	−0.9 (6)	1.6 (6)

[a] Internuclear distances in Å, angles in degrees. Error limits are given in parentheses in units of the last digit.

[b] The structure was calculated from the coordinates based on I_b and I_c (Table 11).

[c] From Kwei and Curl[12].

[d] From Stiefvater[19]. The structure was calculated by fitting the structural parameters to the moments of inertia.

[e] Formic anhydride, from Vaccani, Roos, Bauder and Günthard[22].

[f] Error estimated. This angle was not given in the original reference.

[g] This distance was not reported in Ref. [19].

V. Discussion

The structural parameters of the two rotamers of formic acid are not identical, as is shown in Figs. 2 and 3. Similar changes have been found between the *cis* and *trans* rotamers of monothioformic acid [20] which is also shown in Figure 3.

Although the changes in the structural parameters are in some cases within the error limits (Table 12), we believe these changes to be significant. The most striking changes involve the three angles $\sphericalangle H_1CO_2$, $\sphericalangle CO_2H_2$ and $\sphericalangle O_1CO_2$ and may be attributed largely to repulsion between the hydrogen atoms in the *cis* rotamer. The shortening of the $C{=}O_1$ and $O_2{-}H_2$ distances, the lengthening of the $C{-}O_2$ distance and, in part, the closing of the O_1CO_2 angle, on going from the *trans* to the *cis* rotamer, are consistent with the resonance from I being of greater (albeit small) importance than II, as was also found by *ab initio* calculations [21]. Resonance form I, but not II, may be stabilised through electrostatic attraction of H_2 to the carbonyl oxygen atom O_1.

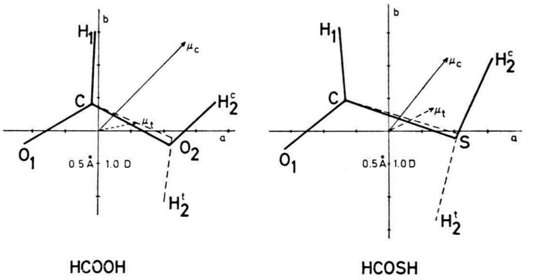

Fig. 3. Comparison of the *cis* and *trans* rotamers of HCOOH and HCOSH. The H_1CO_1 group is unchanged to the accuracy of the drawing when going from *cis* to *trans*. The arrows indicate the positive ends of the dipole moments, μ. The dipole moment data on HCOOH are from Hocking [3]. The HCOSH data are from Hocking and Winnewisser [20], [24].

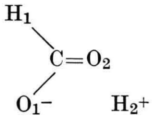

I

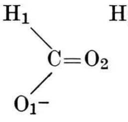

II

Comparison of *cis*-HCOOH with other carboxylic acids is difficult, since a rotamer corresponding to the *cis* form of formic acid has been detected only in special cases, in which it has been stabilised through an intramolecular hydrogen bond, as in glyoxylic acid [18] (HCOCOOH). An interesting comparison is offered by formic anhydride [22] where the preferred conformation may be regarded as consisting of a *cis* and a *trans* half. The differences between these two nonequivalent HCOO groups are consistent with the changes found for formic acid, Table 12.

In Ref. [3] the potential function of the OH torsional vibration was assumed to be of the form:

$$V(\theta) = \tfrac{1}{2} V_1 (1 - \cos\theta) + \tfrac{1}{2} V_2 (1 - \cos 2\theta)$$

where θ is the torsional angle, $\theta = 0°$ in the *trans* rotamer and $\theta = 180°$ in the *cis* rotamer. The (G_{tt}^{-1}) elements were recalculated for the structures reported in Table 12 using Polo's method [23]. The values are $(G_{\text{tt}}^{-1})_{\text{c}} = 0.7109\ \text{u} \cdot \text{Å}^2$ and $(G_{\text{tt}}^{-1})_{\text{t}} = 0.6767\ \text{u} \cdot \text{Å}^2$. Following the procedure in Ref. [3] the revised potential constants are calculated to be:

$$V_1 = 1399\ \text{cm}^{-1}\ (16.7\ \text{kJ/mol},\ 4.0\ \text{kcal/mol}),$$
$$V_2 = 4113\ \text{cm}^{-1}\ (49.2\ \text{kJ/mol},\ 11.8\ \text{kcal/mol}).$$

The barrier to internal rotation as seen from the bottom of the potential well of the *trans* rotamer is: $V_{\max} - V(0) = 4842\ \text{cm}^{-1}$ (58.0 kJ/mol, 13.8 kcal/mol). The torsional vibrational transition of *cis*-HCOOH is predicted to lie at 574 cm^{-1} and the $v = 1 \rightarrow 2$ transition of the *trans* rotamer is predicted at 618 cm^{-1}.

Acknowledgements

The support by the Alexander von Humboldt-Foundation in the form of a fellowship to one of us (E.B.) is gratefully acknowledged. Dr. Gisbert Winnewisser is thanked for providing through his grants the isotopically enriched samples of formic acid. Dr. Koichi Yamada kindly let us use his least squares centrifugal distortion program. Drs. Brenda and Manfred Winnewisser are thanked for their comments on the manuscript and many stimulating discussions.

[1] See Ref. [3] for extensive references to infrared, microwave, electron diffraction and theoretical studies on formic acid.
[2] B. V. Cheney and R. E. Christoffersen, J. Chem. Phys. **56**, 3503 (1972).
[3] W. H. Hocking, Z. Naturforsch. **31a**, 1113 (1976).
[4] T. Miyazawa and K. S. Pitzer, J. Chem. Phys. **30**, 1076 (1959).
[5] I. C. Hisatsune and J. Heicklen, Can. J. Spectrosc. **18**, 135 (1973).
[6] H. Kim, R. Keller, and W. D. Gwinn, J. Chem. Phys. **37**, 2748 (1962).

[7] G. Winnewisser and E. Churchwell, Astrophys. J. (Letters) **200**, L33 (1975).
[8] W. H. Hocking and G. Winnewisser, Z. Naturforsch. **31a**, 422 (1976).
[9] J. K. G. Watson, J. Chem. Phys. **46**, 1935 (1967).
[10] K. Yamada and M. Winnewisser, Z. Naturforsch. **30a**, 672 (1975); erratum ibid, p. 1794.
[11] D. Kivelson and E. B. Wilson, Jr., J. Chem. Phys. **20**, 1575 (1952).
[12] G. Hsing Kwei and R. F. Curl, Jr., J. Chem. Phys. **32**, 1592 (1960).
[13] J. Bellet, A. Deldalle, C. Samson, G. Steenbeckeliers, and R. Wertheimer, J. Mol. Struct. **9**, 65 (1971).
[14] J. Kraitchman, Amer. J. Phys. **21**, 17 (1953).
[15] C. C. Costain, J. Chem. Phys. **29**, 864 (1958).
[16] L. C. Krisher and L. Pierce, J. Chem. Phys. **32**, 1619 (1960).
[17] R. Schwendeman, Structural parameters from rotational spectra, Chapter IIc of Critical Evaluation of Chemical and Physical Structural Information, edited by D. R. Lide, Jr. and M. A. Paul, National Academy of Sciences, Washington D.C. 1974.
[18] B. P. van Eijck and F. B. van Duijneveldt, J. Mol. Struct. **39**, 157 (1977).
[19] O. L. Stiefvater, J. Chem. Phys. **62**, 244 (1975).
[20] W. H. Hocking and G. Winnewisser, Z. Naturforsch. **32a**, 1108 (1977).
[21] M. E. Schwartz, E. F. Hayes, and S. Rothenberg, J. Chem. Phys. **52**, 2011 (1970).
[22] S. Vaccani, U. Roos, A. Bauder, and Hs. H. Günthard, Chem. Phys. **19**, 51 (1977).
[23] S. R. Polo, J. Chem. Phys. **24**, 1133 (1956).
[24] W. H. Hocking and G. Winnewisser, Z. Naturforsch. **31a**, 995 (1976).

Verantwortlich für den Inhalt: A. Klemm
Satz und Druck: Konrad Triltsch, Würzburg